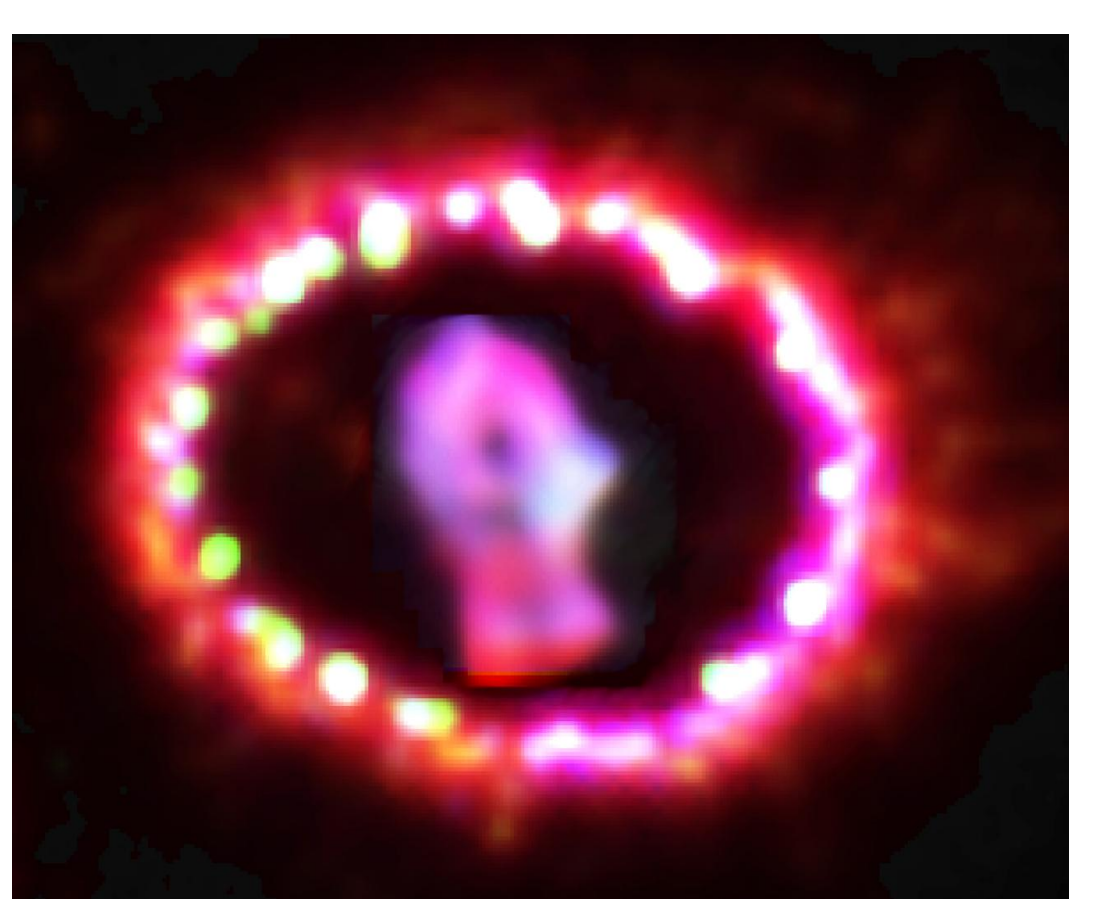
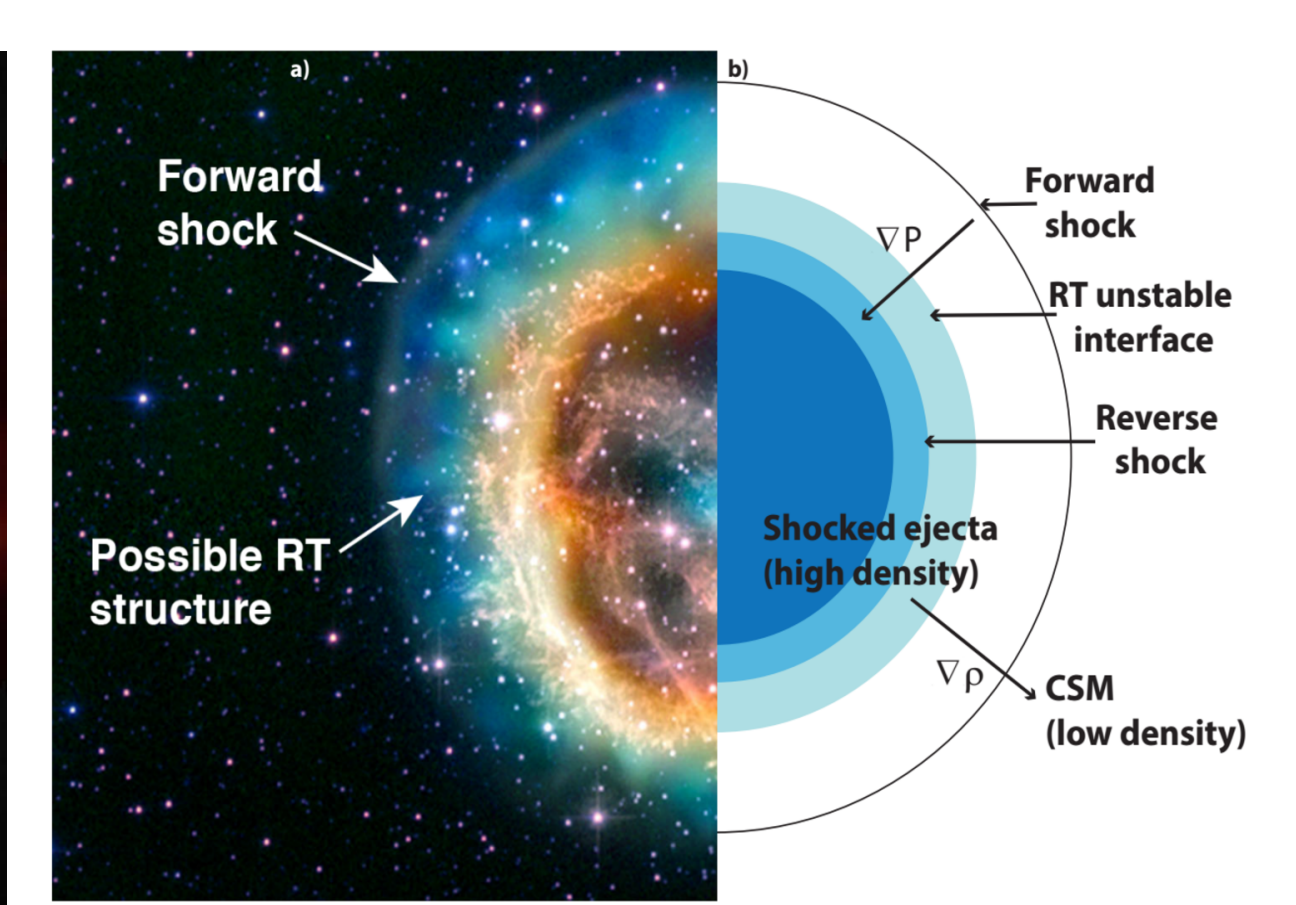


Modeling and Design of Radiative Hydrodynamic Experiments with X-ray Thomson Scattering Measurements on NIF

K.H. Ma¹, H.J. LeFevre¹, P.X. Belancourt ¹, M.J. MacDonald ², T. Doeppner³, P.A. Keiter¹, C.C. Kuranz ¹, E. Johnsen¹ 1 University of Michigan, 2 University of California, Berkeley, 3 Lawrence Livermore National Laboratory

Radiative shocks are present in astrophysical systems

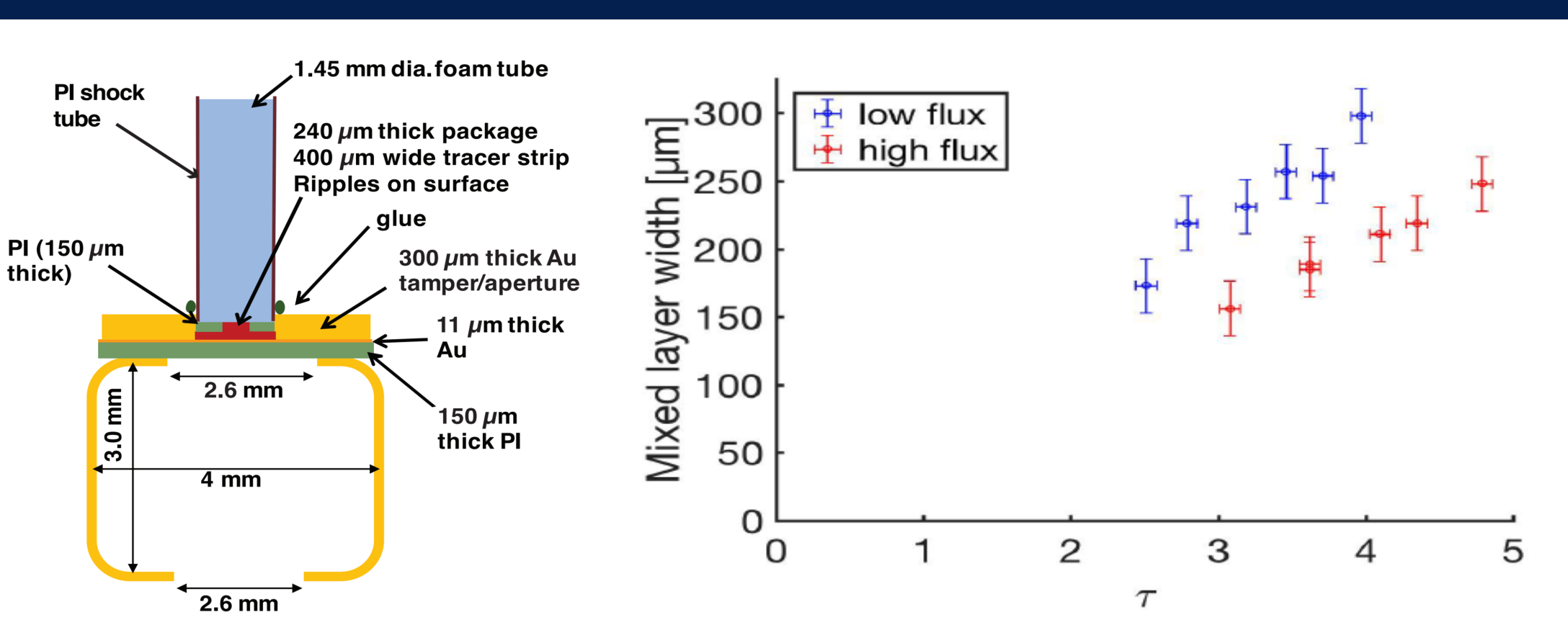




Left: Hubble image of SNR 1987A [1]. Center/Right: False color image of SNR E0102.2-72 [2].

In type II supernovae, core-collapse drives a forward shock into the circumstellar medium (CSM) and a reverse shock into the stellar ejecta, forming a supernova remnant. As stellar mass accumulates in the shocked layer, it decelerates, becoming Rayleigh Taylor unstable. For sufficiently dense CSM, the hot shocked matter produces significant radiative fluxes [3].

We build on a successful NIF radiation hydrodynamics platform [4]



Left: Cross-section of indirect-drive shock tube. Right: Measured mix width of high and low flux shocks vs. non-dimensional growth factor $\tau = \int \gamma_{RT} dt$.

- Previous work studied the effect of radiation on shock-driven hydrodynamic instability growth in indirect drive NIF targets with 20 mg/cc SiO₂ foam.
- X-ray radiography measurements indicate perturbation mix width is lower in highly radiative (compared to non-radiative) shocks.
- It is hypothesized this reduction is due to ablation from higher temperatures in the foam for radiative shocks.

Objective: Implement X-ray Thomson Scattering (XRTS) to measure the temperature in the hot, shocked foam.

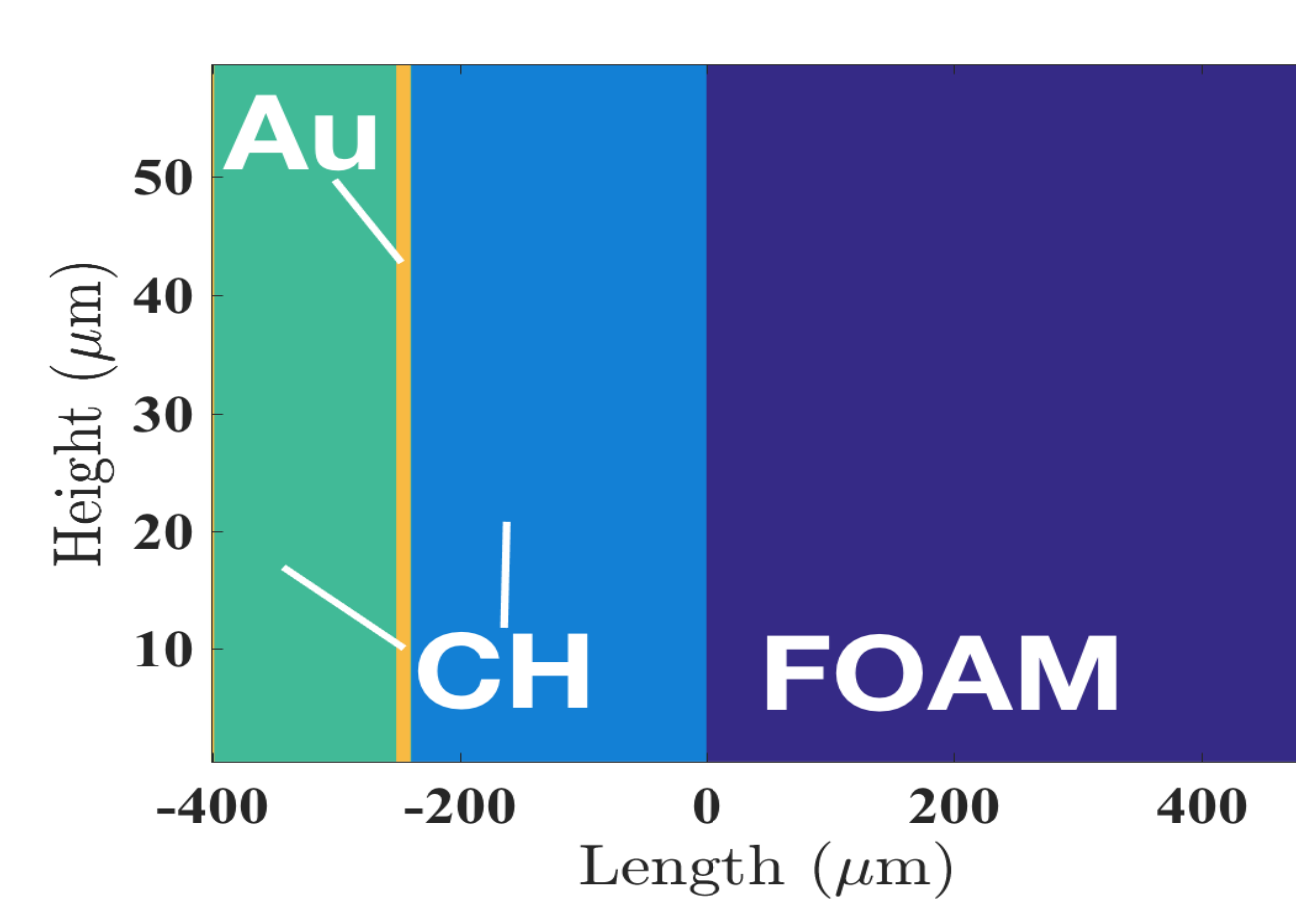
The shocktube is modeled as a 2D planar system

Calculations were performed with CRASH, an Eulerian radiation hydrodynamics code with block-adaptive mesh refinement, multi-group radiation transport and electron heat conduction [5]. Electron conduction heat flux limiter f = 0.06 is used.

Domain composition:

- \bullet 150 μ m of 1.42 g/cc CH (green).
- 11 μ m of 19.3 g/cc Au (gold).
- \bullet 240 μ m of 1.45 g/cc CH (light blue).
- \bullet 4000 μ m of low-density foam (dark blue).

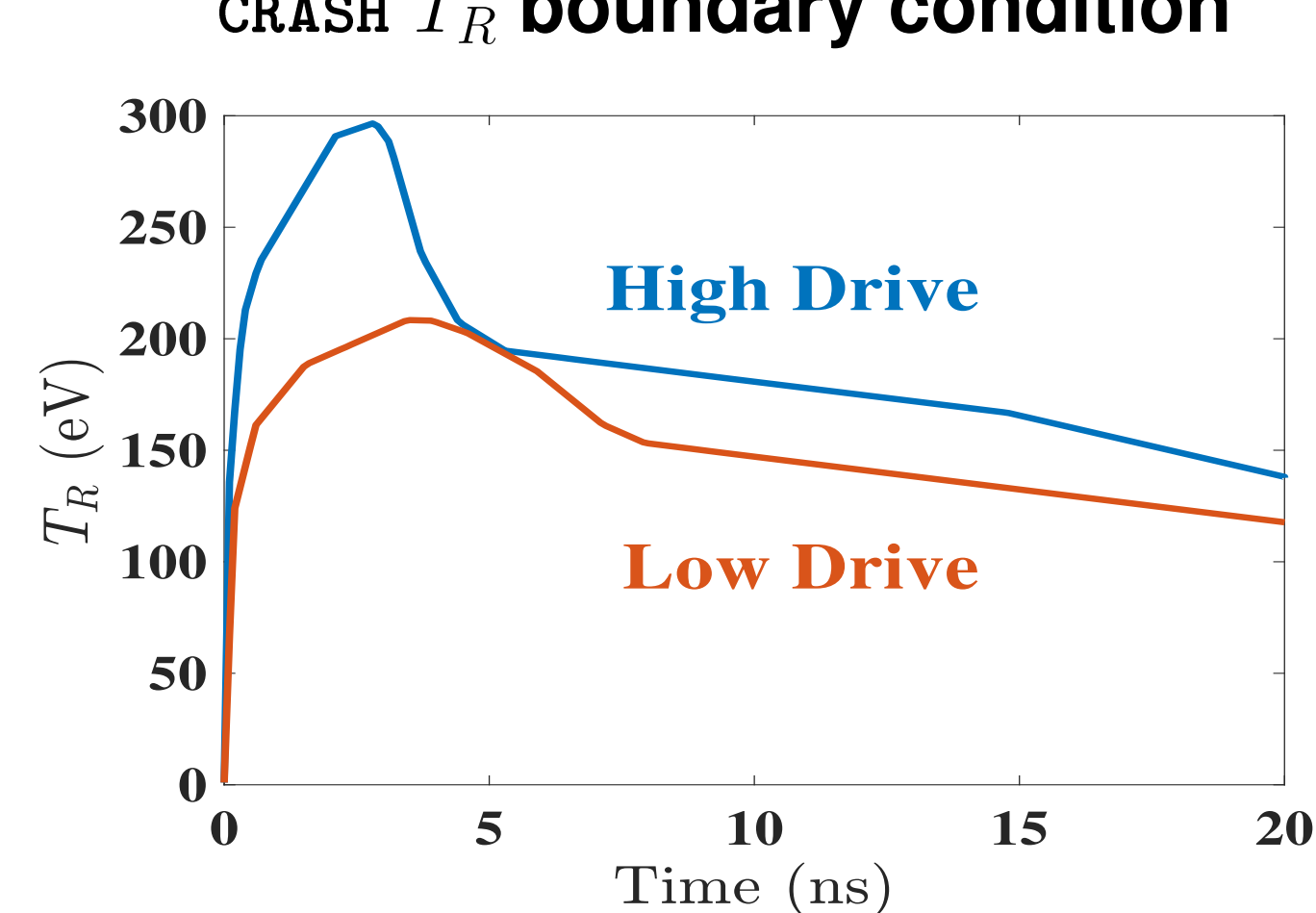
Initialized simulation domain



Drive Condition

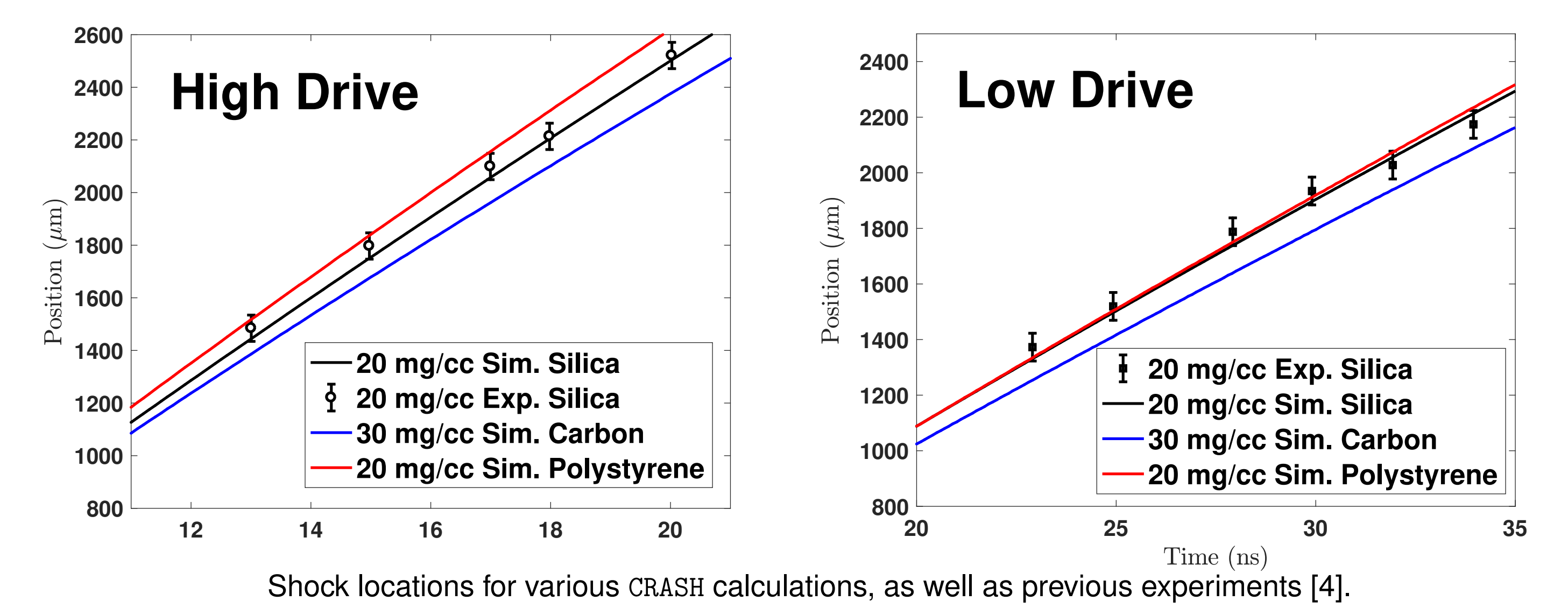
- The indirect drive is modeled with a time-dependent T_R on the left boundary.
- ullet Simulation T_R is lower than experimental values to match shock speeds.

CRASH T_R boundary condition



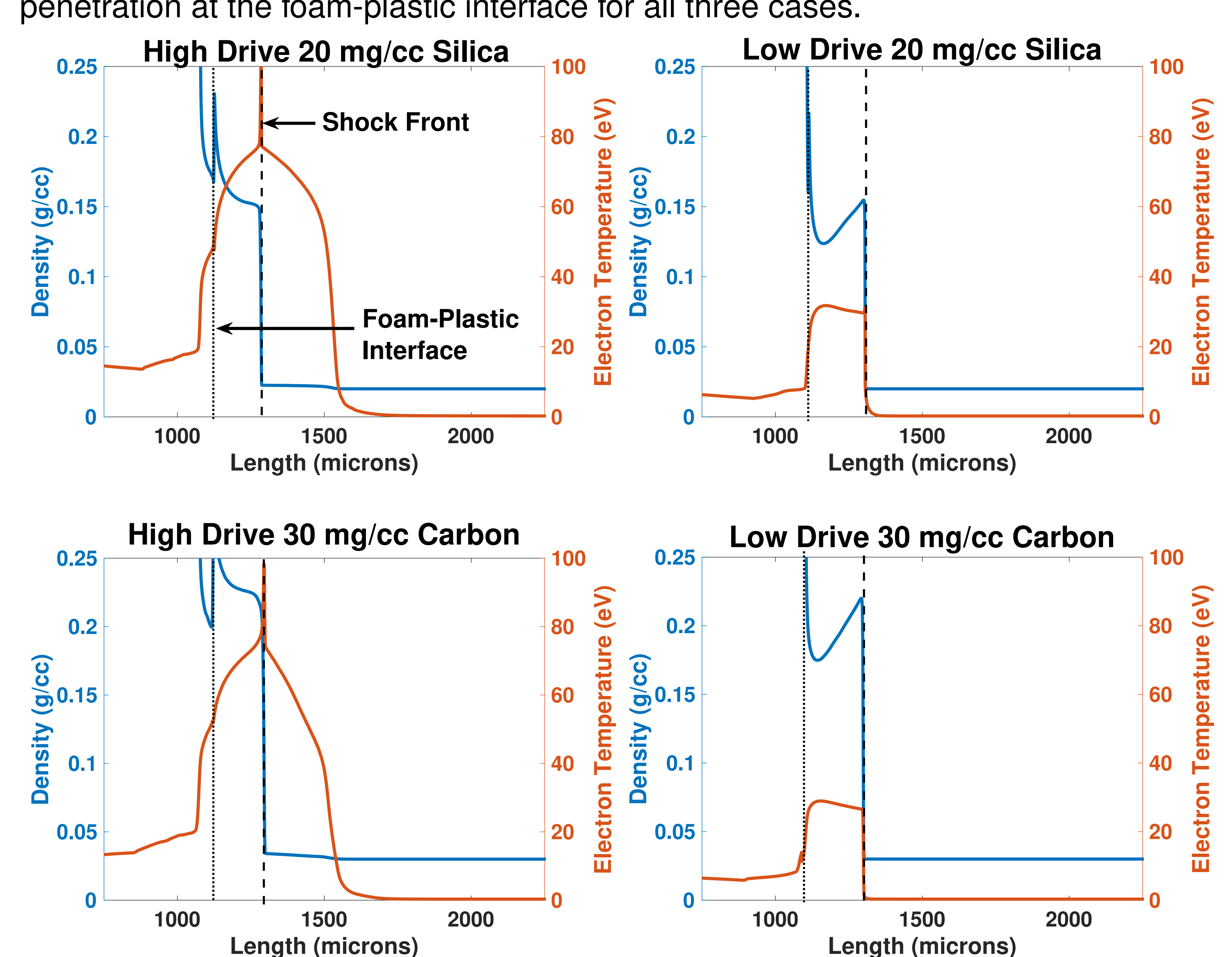
We assessed three materials for the low density foam

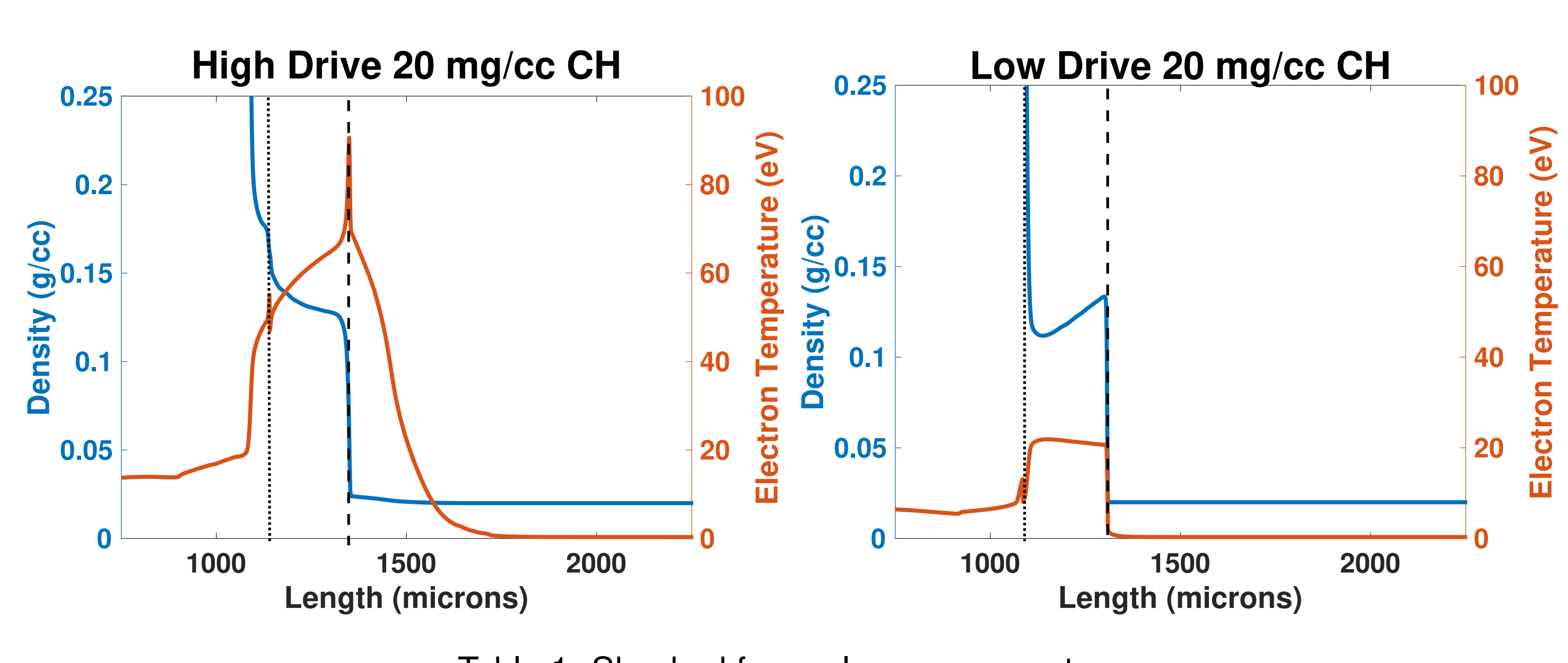
- Shock tube performance with high and low drive was calculated for 20 mg/cc silica (SiO²), 20 mg/cc polystyrene (CH), and 30 mg/cc carbon foam.
- Silica foam simulations match experimentally measured shock locations well.



Radiative precursor characteristics differ for the various materials

Despite variations in the precursor, we see greater thermal energy and heat front penetration at the foam-plastic interface for all three cases.

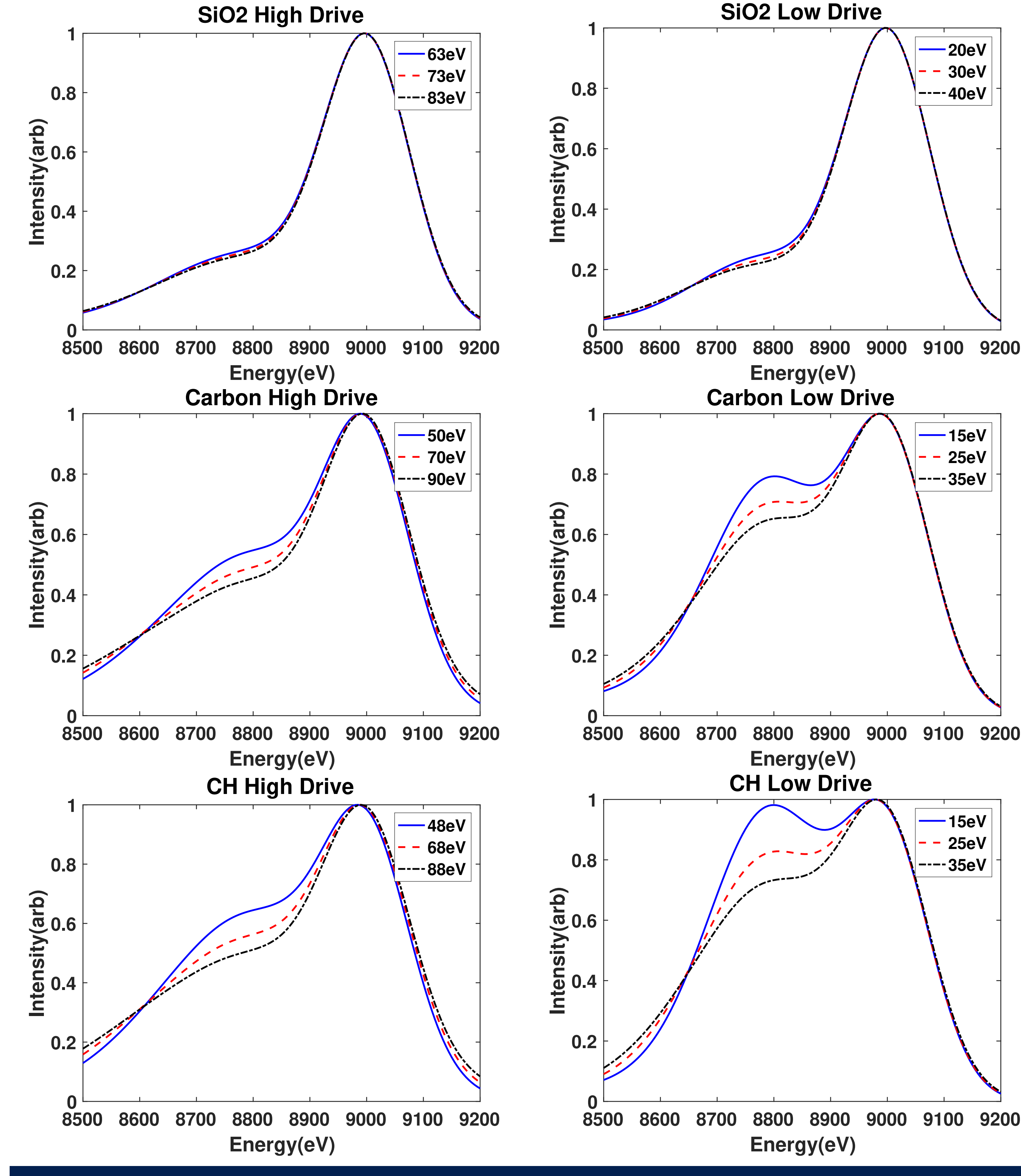




lable 1: Shocked toam plasma parameters							
	Material	SiO_2	Carbon	CH	SiO_2	Carbon	CH
	Initial Density (g/cc)	20	30	20	20	30	20
	Drive	High	High	High	Low	Low	Low
	T_e (eV)	75	70	65	30	25	20
	Ionization (Z)	7	3.5	3	4.5	2.3	2
	u_S (km/s)	125	120	125	70	65	70

XRTS Spectra were generated from CRASH plasma parameters

- ullet Synthetic spectra for the XRTS diagnostic were generated with \pm 10-20 eV [6].
- In SiO₂, the 9 keV peak from elastic scattering of bound electrons is much larger than the Compton peak from free electrons. The Compton peak seems to have a weak temperature dependence.
- The lower Z carbon and CH provide a better measurement for the diagnostic.



Summary

- Indirect X-ray drive shock tubes were modeled with high and low drive for SiO₂, carbon, and CH foams.
- For high drive, characteristics of the radiation precursor profile differs between materials.
- Simulated XRTS spectra were calculated using plasma parameters from CRASH calculations.
- Factoring in diagnostic resolution, 30 mg/cc Carbon foam shows best promise for the XRTS measurement.

Future Work

 Perform photonics estimations to determine XRTS measurement statistics for the Compton peak.

Acknowledgements

This work is funded by the LLNL under subcontract B614207, and was performed under the auspices of the U.S. DOE by LLNL under Contract No. DE-AC52-07NA27344

References

- 1] NASA, ESA, and P. Challis (Harvard-Smithsonian Center for Astrophysics)
- X-ray (NASA/CXC/MIT/D.Dewey et al. & NASA/CXC/SAO/J.DePasquale); Optical (NASA/STScI)
- T.K. Nymark et al., Astron. Astrophys. 449, 171-192 (2006).
- C.C. Kuranz, H.S. Park, et al., Nature Communications (2017). To Be Published. B. van der Holst et al., Astrophys. J. Suppl. Ser. (2011).
- [6] G. Gregori et al., Phys. Plas. 11, 2754 (2004).